THE JOURNAL OF PHYSICAL CHEMISTRY B

Article

pubs.acs.org/JPCB

pH-Dependent Photoreaction Pathway of the All-Trans Form of *Anabaena* Sensory Rhodopsin

Shinya Tahara,[†] Yoshitaka Kato,[‡] Hideki Kandori,[‡] and Hiroyuki Ohtani*[,†]

[†]Department of Bioscience and Biotechnology, Tokyo Institute of Technology, Midori-ku, Yokohama, 226-8501, Japan

[‡]Department of Frontier Materials, Nagoya Institute of Technology, Showa-ku, Nagoya, 466-8555, Japan

ABSTRACT: *Anabaena* sensory rhodopsin (ASR) is well-known as the only retinal protein that achieves the photochromic reaction between the all-trans form (AT-ASR) and the 13-cis form (C-ASR). Although it is known that the structure of the hydrogen-bonding network of ASR is pH-dependent, it is so far unclear how pH affects the photoreaction of ASR. We investigated the pH dependence of the photoreaction of AT-ASR by means of time-resolved absorption spectroscopy and found it to be extremely dependent on pH. At pH 7 and 9, not only the L intermediate but also the K intermediate consisted of two decay components. The formation ratios of the two distinct L intermediates L^{fast}:L^{slow} at pH 7 and 9 were different from each other, although the K^{fast}:K^{slow} ratio was pH-independent. The photoreaction at pH 5 was entirely different from that at pH 7 and 9. Two K intermediates existed, but their formation ratio and lifetimes were different at pH 7 and 9. Moreover, only one L intermediate exists, with a longer lifetime relative to pH 7 and 9. The final product of the photoreaction of AT-ASR was C-ASR at all pH values. Finally, we successfully determined the pH-related photoreaction pathway of AT-ASR.

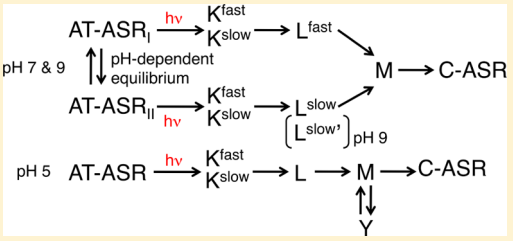

INTRODUCTION

Bacteriorhodopsin (bR) and sensory rhodopsin (sR) belong to the archaeal rhodopsin family.[1,2] bR is the light-driven proton pump and sR works as the light sensor. *Anabaena* sensory rhodopsin (ASR), which is found in the eubacterium *Anabaena* (*Nostoc*) sp. PCC7120, is also a kind of archaeal rhodopsin and is believed to work as a sensor that regulates gene expression by being coupled to 14 kDa soluble transducer in its cell.[3−5]

The structure of ASR is very similar to that of bR, but the replacement of Asp212 in bR with Pro206 is a large difference between them.[6] In addition, ASR has the hydrogen-bonding network from Lys210 to Glu36 on its cytoplasmic side (Figure 1).[6] Recently NMR study showed that not only bR but also ASR forms a trimer in both detergent and membrane.[7]

As with other retinal proteins, light absorption by ASR triggers the photoisomerization of retinal chromophore, and the successive reactions take place within microseconds to milliseconds.[3] In analogy with bR, intermediates named K, L, M, and X are populated in these reaction processes.[1,8,9] The K intermediate is produced within a few picoseconds after excitation of *all-trans*-ASR (AT-ASR).[10] The formation of L and M intermediates follows the decay of the K intermediate. 13-*cis*-ASR (C-ASR) converts to the X intermediate (which corresponds to the ^{610}C intermediate of bR[11] within 1 ps after photoexcitation.[10] Distortion of the retinal chromophore of the K intermediate is localized in the Schiff base region, and the hydrogen bond between the Schiff base and counterion Asp75 is completely disrupted.[12] On the other hand, distortion of the retinal chromophore of the X intermediate is delocalized along the polyene chain and the hydrogen bond of the Schiff base proton is not perfectly disrupted.[13] The properties of these intermediates have been elucidated by means of light-induced current measurement,[14,15] UV−Vis and IR spectroscopy,[8,9,15−17] and transient grating measurement.[18] A previous study showed the M intermediate to be a key phase for physiological function.[18] Therefore, in order to understand physiological function, it is necessary to elucidate the properties of the intermediates as with all other retinal proteins.

In striking contrast to the other retinal proteins, ASR achieves photointerconversion between AT-ASR and C-ASR.[6] The quantum yields for C-ASR from AT-ASR and for AT-ASR from C-ASR conversions are 0.38 and 0.24, respectively.[19] Low-temperature UV−Vis spectroscopy by Kawanabe et al.[20] revealed that AT-ASR converts to C-ASR through K, L, and M intermediates and that C-ASR converts to AT-ASR through X intermediates; namely, the photoreaction of ASR is "complete photochromism" (Figure 2). A previous quantum mechanical/molecular mechanical (QM/MM) calculation suggested that the entire photoreaction of ASR shows a ratchet-like structural change of the retinal chromophore.[21]

The structures of the hydrogen-bonding network of ground-state ASR and intermediates are pH-dependent. Shi et al.[9] and Bergo et al.[16] reported that the formation of M intermediate includes protonation of the Asp217 carboxyl group, while the acceptor of the Schiff base proton of bR is Asp85 (which corresponds to Asp75 of ASR). Shi et al.[9] also clarified that Asp217 is protonated at pH 5 even in an unphotolyzed state. Moreover, Kawanabe et al.[17] showed that Glu36 is protonated

Received: November 13, 2012
Revised: January 22, 2013
Published: January 28, 2013

   dx.doi.org/10.1021/jp311217a | *J. Phys. Chem. B* 2013, 117, 2053−2060

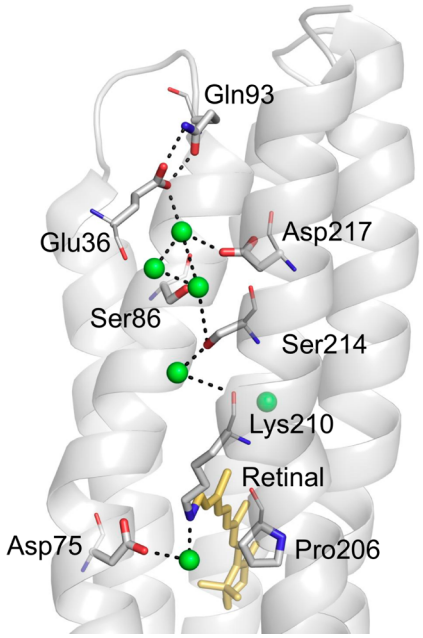

Figure 1. X-ray crystallographic structure of the cytoplasmic region of ASR (PDB entry 1XIO).[6] Top and bottom regions correspond to the cytoplasmic surface and retinal binding pocket, respectively. Internal water molecules are shown by green spheres, and hydrogen bonds (---) are inferred from the structure.

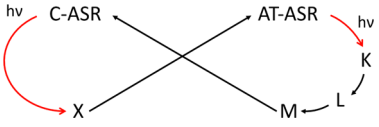

Figure 2. "Complete photochromism" for ASR, as proposed by Kawanabe et al.[20].

at pH 5 in ground-state ASR and that the L intermediate is deprotonated at pH 9. pK_a values of the carboxyl groups of Asp217 and Glu36 were suggested to be between 6 and 7.

Sineshchekov et al.[8] examined the pH dependence of the rise and decay times of the M intermediate. As a result, pK_a values for the decay and rise of the M intermediate are 6.3 and 8.0, respectively. The pH dependence of the lifetimes of intermediates allows us to assume that the reactions of the retinal chromophore are controlled by alterations in pH.

In this study, we examined the photoreaction of AT-ASR in detail by means of steady-state UV−Vis absorption spectroscopy and time-resolved absorption spectroscopy at different pH values. Unlike previous reports, not only two L intermediates but also two K intermediates were discovered. A pH dependence of the ratios of their yields, K^{fast}:K^{slow} and L^{fast}:L^{slow}, was revealed. A pH dependence of the absorption spectra of the ground-state ASR and intermediates was also shown. Finally, pH-dependent photoreaction pathways of AT-ASR are proposed.

MATERIALS AND METHODS

Sample Preparation. We prepared the full-length ASR in accordance with a method described elsewhere.[3,20] Briefly, the C-terminally His-tagged full-length ASR was expressed by *Escherichia coli* BL21 strain. The cells were harvested and sonicated. The ASR protein was solubilized with 1% *n*-dodecyl *β*-D-maltoside (DDM) and purified by a Ni^{2+}−nitrilotriacetic acid (NTA) column. The purified ASR solution was dialyzed. The dialysates were 25 mM 1,4-piperazinediethanesulfonic acid (PIPES) buffer for pH 7, 25 mM boric acid buffer for pH 9, and 25 mM citric acid buffer for pH 5. These buffer solutions contained 200 mM NaCl and 0.2% DDM.

Steady-State UV−Vis Absorption Spectroscopy. A commercial UV−Vis spectrometer (V570, Jasco) with an integrating sphere component (ISN-470, Jasco) was used to measure the absorption spectra of ground-state ASR solutions at room temperature.

Time-Resolved Absorption Spectroscopy. Two complementary measurements, kinetic spectroscopy (Figure 3a) and pump−probe spectroscopy (Figure 3b), were performed. The former provides the time dependence of transient absorption at a selected wavelength, while the latter provides a time-resolved absorption spectrum at a selected delay time. The second harmonic of a Q-switched Nd^{3+}:YAG laser (5 ns full width at half-maximum, fwhm; Minilite I, Hoya-Continuum) was used for the excitation light source of the two measurements.

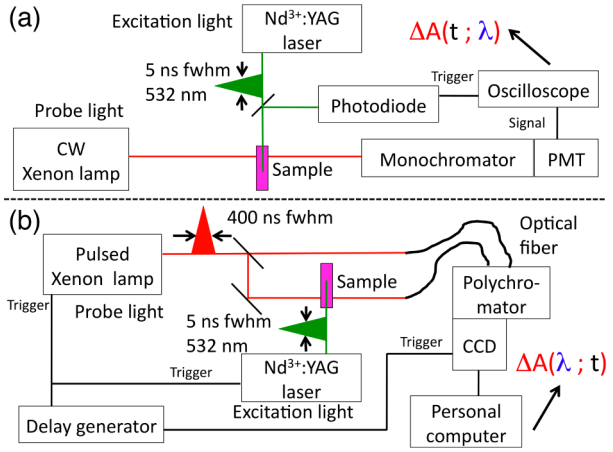

Figure 3. Apparatus for time-resolved absorption spectroscopy. (a) Kinetics spectroscopy for measurement of $\Delta A(t)$ at λ. (b) Pump−probe spectroscopy for measurement of $\Delta A(\lambda)$ at t.

For kinetic spectroscopy, a continuous-wave (CW) xenon lamp [150 W; L2274, Hamamatsu Photonics K.K. (HPK)] was used as the probe light source. The transmitted probe light from the sample was dispersed by a monochromator (f = 100 mm, 600 grooves/mm, CT-10, Jasco) and detected by a photomultiplier tube (R3825, HPK). The output from the photomutiplier tube was monitored by an oscilloscope (DPO3054, Tektronix). For pump−probe spectroscopy, a pulsed xenon lamp (400 ns fwhm, HPK) was used as the probe light source. The transmitted probe light was dispersed by a polychromator (f = 250 mm, 300 grooves/mm, MS257, Oriel Instruments) and detected by a cooled charge-coupled device (CCD) camera system (Newton, Andor Technology).

RESULTS

Absorption Spectra of Ground-State *Anabaena* Sensory Rhodopsin at pH 7, 9, and 5. Figure 4 shows the absorption spectra of ground-state ASR samples. Dark-adapted (DA) samples were prepared by maintaining samples in the dark for 24 h at room temperature before measurement of the absorption spectra. Spectra of the light-adapted (LA) samples were measured after irradiation of the DA samples with

dx.doi.org/10.1021/jp311217a | J. Phys. Chem. B 2013, 117, 2053−2060

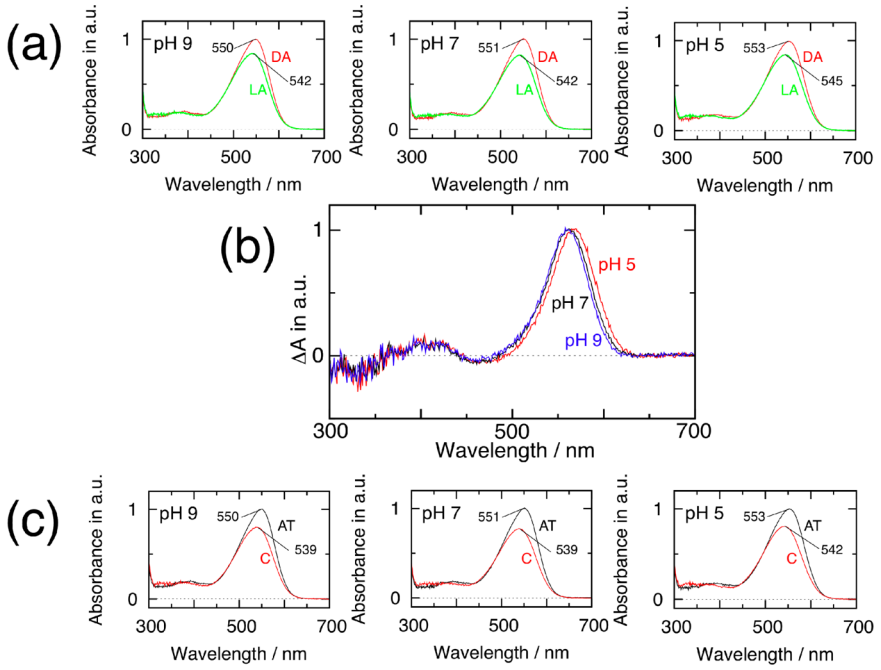

Figure 4. Absorption spectra of ground-state ASR samples at pH 7, 9, and 5. (a) Dark-adapted (DA) and light-adapted (LA) samples. (b) Difference spectra between DA and LA samples. (c) Calculated spectra of AT-ASR and C-ASR. The isomeric composition reported by Kawanabe et al.[20] was applied to these calculations at all pH values.

orange light (λ > 560 nm) for 5 min. DA and LA samples at pH 9 show only 1−3 nm blue-shifted spectra compared to those at pH 7. Unlike at pH 9, the samples at pH 5 exhibited 3−5 nm red-shifted spectra.

The AT-ASR minus C-ASR difference spectra at pH 7, 9, and 5 were obtained by subtracting LA spectra from DA. These spectra at pH 7 and 9 (Figure 4b) are slightly different from each other, but only the spectra at pH 5 are red-shifted 3−5 nm from them. From these results, we concluded that AT-ASR and C-ASR spectra at pH 7, 9, and 5 are different from each other.

AT-ASR and C-ASR spectra were calculated from the isomeric composition obtained from HPLC analysis conducted by Kawanabe et al.[20] (Figure 4c).

Lifetimes of *Anabaena* Sensory Rhodopsin Intermediates. The lifetimes (1/e lifetime) were obtained from kinetic traces of the 350−650 nm wavelength region. The kinetics was well fitted as a sum of single-exponential functions. The successive fitting of the slowest component of the kinetics by a single exponential and subtraction of it from the kinetics yielded the lifetimes (and relative yields) of the all intermediates. These lifetimes and their assignments to intermediates are shown in Figure 5 and Table. 1.

The lifetimes measured at pH 7 are almost the same as those reported previously, except for the lifetime of K intermediates.[8,18] Earlier studies showed that the K intermediate consists of only one component with a 70−100 μs lifetime,[8,18] although two K intermediates, K^{fast} and K^{slow}, with 30 and 300 μs lifetimes, respectively, were found. As Sineshchekov et al.[8] reported, we also found two L intermediates, L^{fast} and L^{slow}, with lifetimes of 1 and 8 ms, respectively.

The lifetimes of all intermediates at pH 9 are identical to those at pH 7 except for X intermediates.

At pH 5, not only the ground-state ASR spectra but also the lifetimes of intermediates are entirely different from those measured at pH 7 and 9. Two transient species assigned to K intermediates appeared, but their lifetimes were 10 times longer

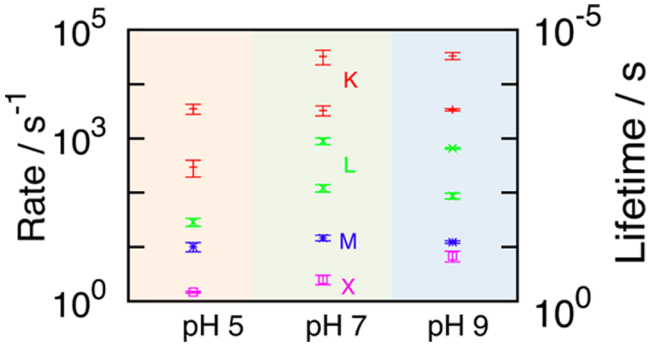

Figure 5. Effect of pH on lifetimes of ASR intermediates at each pH value.

(300 μs and 3 ms, respectively) than those at pH 7 and 9. Moreover, the L intermediate consists of only one component with a 30 ms lifetime at pH 5, unlike at pH 7 and 9. The lifetime of the M intermediate at pH 5 was slightly longer than at pH 7 and 9.

The lifetime of the X intermediate increased as pH decreased.

Absorption Spectra of K and L Intermediates. Difference spectra between L and K intermediates (L − K spectra) were calculated from time-resolved absorption spectra (Figure 6a). Contributions from the C-ASR photoreaction could be offset by scaling and subtracting the time-resolved absorption spectra. The scaling factors were calculated from the lifetimes of the X intermediate. The obtained L − K^{fast} and L − K^{slow} spectra were identical to each other at all pH conditions, but the L − K spectra at pH 5 were red-shifted from those at pH 7 and 9.

Figure 6b shows M − L spectra at pH 7, 9, and 5. The spectra at pH 7 and 9 were obtained from the amplitude of the decaying components with lifetimes of two L intermediates at

dx.doi.org/10.1021/jp311217a | J. Phys. Chem. B 2013, 117, 2053−2060

Table 1. Lifetimes of Intermediates

	K		L		M	X
	$\tau_1/\mu s$	$\tau_2/\mu s$	τ_3/ms	τ_4/ms	τ_5/ms	τ_6/ms
pH 9	43 ± 4	300 ± 14	1.5 ± 0.1	11 ± 2	81 ± 5	150 ± 40
pH 7	31 ± 7	300 ± 50	1.1 ± 0.2	8.2 ± 1.5	68 ± 9	400 ± 100
pH 5	280 ± 50	3400 ± 900	35 ± 7		99 ± 16	681 ± 23

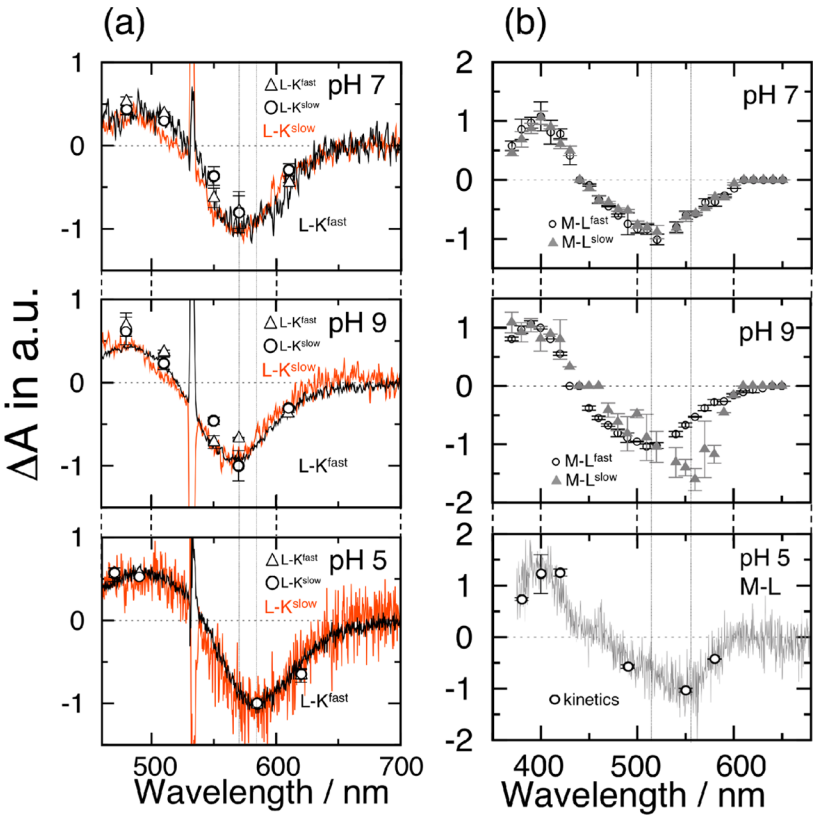

Figure 6. (a) Normalized L minus K (L − K) difference spectra. Solid lines show the calculated spectra from the time-resolved absorption spectra. Triangles and circles indicate the normalized amplitude of the decaying components with corresponding time constants at typical wavelengths. (b) Normalized M minus L (M − L) difference spectra. Spectra of M − L at pH 7 and 9 were calculated from kinetic traces measured at 10-nm intervals. The calculated normalized M − L spectrum from time-resolved absorption spectra at pH 5 (bottom) is displayed by a solid line. Circles indicate the normalized amplitude of the decaying components with a corresponding time constant at typical wavelengths.

respective wavelengths. M − L spectra at pH 7 and M − L^{fast} spectra at pH 9 are identical to each other. M − L^{slow} at pH 9 resembles M − L at pH 5.

Table 2 shows the estimated properties of absorption spectra of K and L intermediates at pH 7, 9, and 5. The estimated spectrum of the L intermediate at pH 5 and that of the L^{slow} intermediate at pH 9 is ∼1000 cm^{-1} red-shifted from L^{fast} and L^{slow} at pH 7 and from the L^{fast} intermediate at pH 9 (Table 2). The red-shifted L − K spectrum at pH 5 may be due to the red shift of the absorption spectrum of the L intermediate. The L^{slow} spectrum at pH 9 is also different from that at pH 7, but their L − K spectra are in good agreement. This originates in low yield of L^{slow} at pH 9 (see below).

Table 2. Wavelengths at Maximum and at Half-Maximum of Absorption Spectra of K and L

species	λ_{max}/nm	$\lambda_{half\ max}$/nm
K^{fast}, K^{slow}	560−570	600−610
pH 7 L^{fast}, pH 7 L^{slow}, pH 9 L^{fast}	510−520	570−580
pH 9 L^{slow}, pH 5 L	550−560	580

Yields of K and L Intermediates (K^{fast}:K^{slow} and L^{fast}:L^{slow}). The kinetic traces in Figure 7 were obtained by subtraction of the slower decaying components from the original kinetics. From the amplitudes of these kinetic traces, we calculated the ratios K^{fast}:K^{slow} and L^{fast}:L^{slow} at pH 7, 9, and 5 (Table 3). The ratio K^{fast}:K^{slow} at pH 7 was identical to that at pH 9, but the relative yield of the L^{fast} intermediate for L^{slow} at pH 9 was much higher than that at pH 7. Note that because of the spectral difference between L^{fast} and L^{slow} (see Figure 6), we estimated their yields from the kinetic traces at wavelengths corresponding to the formation of the M intermediate. K^{fast}:K^{slow} at pH 5 is 3:1, whereas that at pH 7 and 9 is 1:1.

Decay Process of M Intermediate at pH 7 and 9. Figure 8 shows the spectra of the decaying component with 70 ms time constant at pH 7 and 9. These spectra correspond to the difference spectrum between the M intermediate and its product. As the M intermediate has no absorption in the >500 nm wavelength region, the spectrum in the longer wavelength region gives the spectrum of its product. These spectral shapes

dx.doi.org/10.1021/jp311217a | J. Phys. Chem. B 2013, 117, 2053−2060

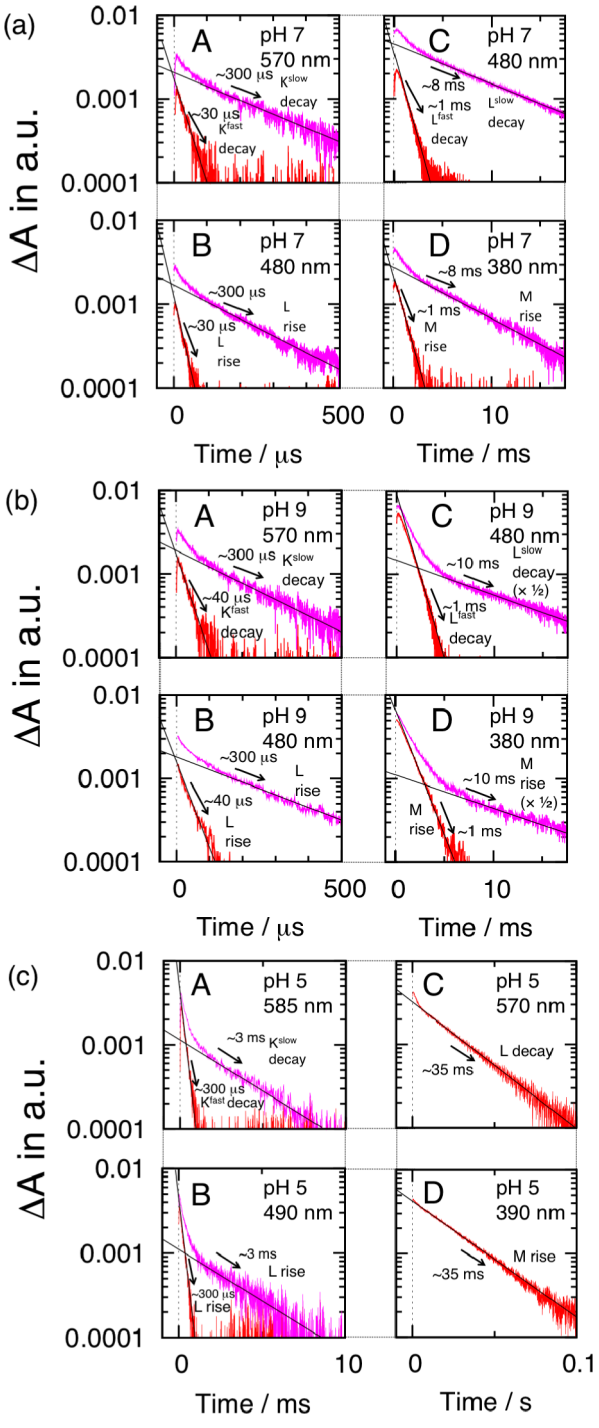

Figure 7. Kinetic traces corresponding to decay or formation of K and L intermediates at (a) pH 7, (b) pH 9, and (c) pH 5. Note that 10 ms components in panel b are drawn to half-scale.

Table 3. Ratios K^{fast}:K^{slow} and L^{fast}:L^{slow} at All pH Values

	K^{fast}:K^{slow}	L^{fast}:L^{slow}
pH 7	1:1	1:1
pH 9	1:1	3:1−5:1
pH 5	3:1	

in the >500 nm wavelength region agree with the absorption spectrum of C-ASR rather than that of AT-ASR. We concluded that the M intermediate does not relax to AT-ASR but to C-ASR. These results support a previous report about the photochromic reaction of ASR by means of low-temperature absorption spectroscopy.[20]

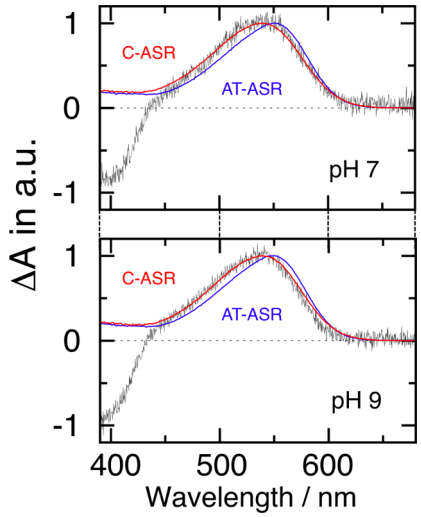

Figure 8. Difference spectra between M intermediate and its product at pH 7 and 9.

Decay Process of M Intermediate at pH 5. Unlike at pH 7 and 9, the difference spectrum of the M intermediate and its product at pH 5 (Figure 9a, orange solid line) in the >500 nm wavelength region agrees with neither the spectrum of C-ASR nor that of AT-ASR at ambient temperature. However, the difference spectrum was temperature-dependent. The amplitude at 480 nm relative to 400 nm changed significantly between 30 and 40 °C (Figure 9b). We measured the difference

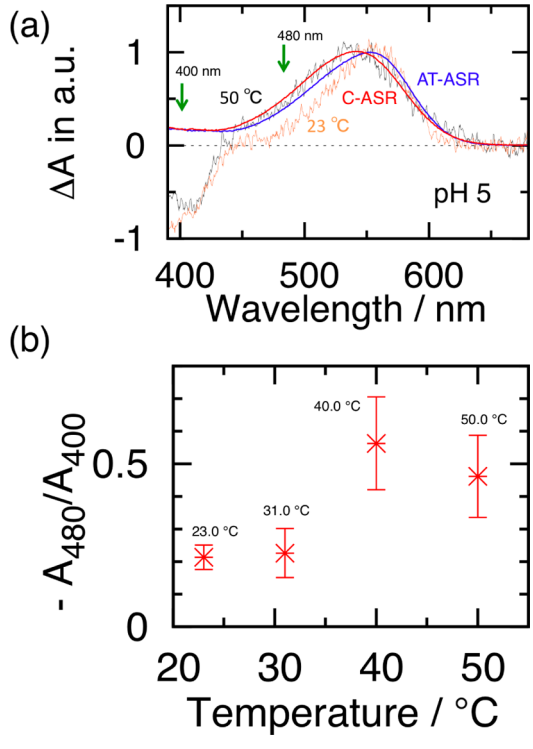

Figure 9. (a) Temperature-dependent difference spectrum between the M intermediate and its product at pH 5. (b) Ratio of the amplitude of kinetic traces with 100 ms time constant at 480 nm relative to 400 nm.

dx.doi.org/10.1021/jp311217a | J. Phys. Chem. B 2013, 117, 2053−2060

spectrum at 50 °C and obtained a spectrum (Figure 9a, black solid line) that is similar to that of C-ASR in the >500 nm region. Thus, we concluded that the product from the M intermediate at pH 5 was also C-ASR, along with those at pH 7 and 9.

DISCUSSION

This study shows that the photoreaction of AT-ASR is extremely dependent on pH. The photoreaction pathway of AT-ASR is discussed next.

Photoreaction of *all-trans Anabaena* Sensory Rhodopsin at pH 7 and 9. First, we discuss the experimental results at pH 7 and 9. The following are the experimental results at pH 7 and 9.

(1) Only one M intermediate appeared at pH 7 and 9. The product of the M intermediate was C-ASR at both pH values.
(2) Two L intermediates, L^{fast} and L^{slow}, were found at pH 7 and 9. Their lifetimes at pH 7 and 9 were identical, but the formation ratios L^{fast}:L^{slow} at pH 7 and 9 were different. Both L intermediates decayed to the single M intermediate.
(3) The absorption spectra of L^{fast} and L^{slow} at pH 7 and L^{fast} at pH 9 were identical to each other, but the absorption spectrum of L^{slow} at pH 9 was red-shifted from them.
(4) Not only L intermediates but also the K intermediate consisted of two components, K^{fast} and K^{slow}. The lifetimes of these intermediates at pH 7 and 9 were identical. The ratios K^{fast}:K^{slow} at pH 7 and 9 were also identical to each other. Each K intermediate yielded L^{fast} and L^{slow}.
(5) The absorption spectra of ground-state ASR at pH 9 were slightly different from those at pH 7 (at pH 9, 1−3 nm blue-shifted from those at pH 7).

From result 1, only one M intermediate exists at pH 7 and 9. This M intermediate converts to C-ASR. Results 2 and 4 imply that not only L intermediates but also K intermediates consist of two components. The existence of the two L intermediates indicates that the reaction pathway bifurcates at K intermediates or before the formation of K. If we assume that the formation of L intermediates from K intermediates is a branching reaction, it is expected that the lifetimes of K^{fast} and K^{slow} at 9 are different from those at pH 7. However, result 4 shows that the lifetimes of K^{fast} and K^{slow} at pH 7 and 9 are identical. Thus, it is insupportable that K^{fast} and K^{slow} bifurcate to two different L intermediates, L^{fast} and L^{slow}. Accordingly, we concluded that the branching of the reaction pathway exists before the formation of the K intermediates. In addition, results 2 and 4 show that L^{fast}:L^{slow} at pH 7 and 9 are different from each other, while K^{fast}:K^{slow} are not. This indicates that the formation of two L intermediates, L^{fast} and L^{slow}, from two K intermediates, K^{fast} and K^{slow}, is not a one-to-one reaction. Considering all results together, we propose a model for the photoreaction pathway of AT-ASR at pH 7 and 9 in Figure 10.

In Figure 10, L^{slow} at pH 9 is denoted by $L^{slow'}$ to emphasize the disagreement of the spectrum with L^{slow} at pH 7. We considered that two distinct structures for the ground-state ASR exist, AT-ASR_I and AT-ASR_{II}. The compositions of these ground-state ASRs at pH 7 and 9 are different from each other. This model is consistent with result 5. The pH change may cause the composition of the two ground-state ASRs, AT-ASR_I and AT-ASR_{II}.

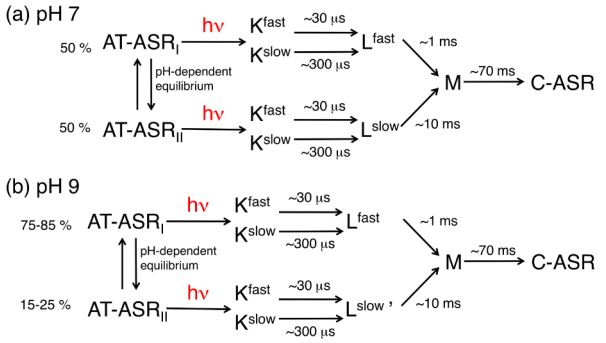

Figure 10. Photoreaction pathway of AT-ASR at (a) pH 7 and (b) pH 9.

Note that the conditions except for pH may affect the measurements by Sineshchekov et al.,[8] which showed that the decrease in pH shortens the formation time of the M intermediate, because they measured the pH effect on ASR not in detergent but in intact *E. coli* cells. Nevertheless, the existence of a proton acceptor with a pK_a between 7 and 9 is unanimous as reported by Sineshchekov et al.,[8] because our result shows that the yield of L^{fast} increases with an increase in pH (without decreasing the lifetime of L intermediates).

According to the infrared-spectroscopic study, the hydrogen bond of Asp217 is not altered until the formation of the L intermediates, but the decay of L intermediates includes protonation of Asp217 with deprotonation of the Schiff base. Our result shows that the protonation/deprotonation of the unknown proton acceptor with pK_a between 7 and 9 has little or no effect on the absorption spectrum of ground-state ASR and the decay process of K intermediates, but it does have an effect on the decay kinetics of L intermediates. Thus, an unknown proton acceptor, which may be a carboxylate, other functional moiety of side-chain residue, or an internal water molecule, is probably involved in the hydrogen-bonding network or related to the network.

The formation of the two components of K, K^{fast} and K^{slow}, implies the existence of an excited-state bifurcation or of multiple structures of the ground-state ASR. Vogeley et al.[6] found two distinct conformations of Lys210 in ground-state ASR, but the relevance of our finding is unclear. In this case, four kinds of ground-state ASRs are present in all. However, we cannot rule out excited-state branching.

From result 3, the chromophore of L^{slow} at pH 9 was placed under a distinct environment from the L intermediates at pH 7 and L^{fast} at pH 9. In general, the absorption spectrum of the retinal chromophore is controlled by the distance between the Schiff base proton and the counterion and by the distribution of charge on the cavity surface.[22−25] However, it is so far unclear how the interaction between chromophore and protein at $L^{slow'}$ differs from the L^{fast} intermediate.

Photoreaction of *all-trans Anabaena* Sensory Rhodopsin at pH 5. The following are our results at pH 5.

(6) Only one M intermediate with a longer lifetime (~100 ms) than that at pH 7 and 9 appeared. The product of the M intermediate was C-ASR at pH 5.
(7) Only one L intermediate with a lifetime (~30 ms) longer than those at pH 7 and 9 existed.
(8) The absorption spectrum of the L intermediate was red-shifted from those of the L intermediates at pH 7 and

dx.doi.org/10.1021/jp311217a | J. Phys. Chem. B 2013, 117, 2053−2060

L^{fast} at pH 9. The spectrum of the L intermediate at pH 5 was in good agreement with $L^{slow'}$ at pH 9.

(9) Two K intermediates, K^{fast} and K^{slow}, were found. Their lifetimes were 10-fold longer (K^{fast} ~300 μs, K^{slow} ~3 ms) than those at pH 7 and 9. The formation ratio K^{fast}:K^{slow} was 3:1.

(10) The spectrum of the decaying component with the lifetime of the M intermediate was temperature-dependent.

(11) The absorption spectrum of ground-state ASR was 3−5 nm red-shifted from that at pH 7.

From results 6 and 7, not only the M intermediate but also the L intermediate consists of only one component. Result 9 shows the presence of two K intermediates. Result 10 indicates that species with an identical lifetime to the M intermediate are present. We propose a photoreaction pathway at pH 5 in Figure 11.

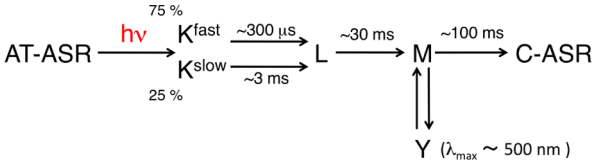

Figure 11. Photoreaction pathway of AT-ASR at pH 5.

The elongated lifetime of the M intermediate at pH 5 is consistent with the report of Sineshchekov et al.[15] From the temperature dependence of the decay of M intermediate, we tentatively suppose that a new intermediate Y is held in equilibrium with M. The absorption wavelength of the Y intermediate is considered to be about 500 nm. At pH 7, the reaction process from M intermediate to C-ASR requires both the reprotonation of the Schiff base and ^{15}C=N isomerization. The Y intermediate is perhaps the product of the M intermediate, which is a reprotonated but not an isomerized species (which corresponds to the N intermediate of bR).

Results 8 and 11 show that the spectra of ground-state ASR and L intermediate are different from those at pH 7. A previous theoretical study shows that the D217N mutation causes an increase of electrostatic potential around the chromophore and a red shift of the AT-ASR spectrum by 27 nm (~800 cm^{-1}) and of the C-ASR spectrum by 17 nm (~600 cm^{-1}), even though Asp217 is a noncavity residue.[26] When this report is considered, it is possible that the structural change of the hydrogen-bonding network attributed to the protonation of Asp217 has the ability to affect the absorption spectra of the ground state or intermediates. It is well-known that bR_{568} is converted to a red-shifted species bR_{605} at low pH, and that its intermediates K_{acid} and L_{acid} also exhibit spectra in the wavelength region longer than those of K and L, respectively.[27−29] The protonation of Asp217 may make the absorption spectra shift to a longer wavelength region via a conformation change in ASR protein rather than through direct interaction with the chromophore. Nevertheless, it cannot be denied that protonation of the additional unknown proton acceptors affects the absorption spectra and decay dynamics. Structural information on the ASR proteins at different pH conditions is required to account for pH dependence of ground-state ASR and intermediate spectra at different pH conditions.

AUTHOR INFORMATION

Corresponding Author

*Phone +81-045-924-5786; fax +81-045-924-5816; e-mail hohtani@bio.titech.ac.jp.

Notes

The authors declare no competing financial interest.

ACKNOWLEDGMENTS

We thank Dr. Akira Kawanabe for his contribution to the launch and development of the research of *Anabaena* sensory rhodopsin in Kandori's laboratory.

REFERENCES

(1) Lozier, R. H.; Bogomolni, R. A.; Stoeckenius, W. Bacteriorhodopsin: A Light-driven Proton Pump in *Halobacterium halobium*. *Biophys. J.* **1975**, *15*, 955−962.

(2) Spudich, J. L.; Bogomolni, R. A. Mechanism of Colour Discrimination by a Bacterial Sensory Rhodopsin. *Nature* **1984**, *312*, 509−513.

(3) Jung, K. H.; Trivedi, V. D.; Spudich, J. L. Demonstration of a Sensory Rhodopsin in Eubacteria. *Mol. Microbiol.* **2003**, *47*, 1513−1522.

(4) Wang, S.; Kim, S. Y.; Jung, K. H.; Ladizhansky, V.; Brown, L. S. A Eukaryotic-Like Interaction of Soluble Cyanobacterial Sensory Rhodopsin Transducer with DNA. *J. Mol. Biol.* **2011**, *411*, 449−462.

(5) Irieda, H.; Morita, T.; Maki, K.; Homma, M.; Aiba, H.; Sudo, Y. Photo-induced Regulation of the Chromatic Adaptive Gene Expression by *Anabaena* Sensory Rhodopsin. *J. Biol. Chem.* **2012**, *287*, 32485−32493.

(6) Vogeley, L.; Sineshchekov, O. A.; Trivedi, V. D.; Sasaki, J.; Spudich, J. L.; Luecke, H. *Anabaena* Sensory Rhodopsin: A Photochromic Color Sensor at 2.0 Å. *Science* **2004**, *306*, 1390−1393.

(7) Wang, S.; Munro, R. A.; Kim, S. Y.; Jung, K. H.; Brown, L. S.; Ladizhansky, V. Paramagnetic Relaxation Enhancement Reveals Oligomerization Interface of a Membrane Protein. *J. Am. Chem. Soc.* **2012**, *134*, 16995−16998.

(8) Sineshchekov, O. A.; Trivedi, V. D.; Sasaki, J.; Spudich, J. L. Photochromicity of *Anabaena* Sensory Rhodopsin, an Atypical Microbial Receptor with a Cis-retinal Light-adapted Form. *J. Biol. Chem.* **2005**, *280*, 14663−14668.

(9) Shi, L.; Yoon, S. R.; Bezerra, A. G., Jr.; Jung, K. H.; Brown, L. S. Cytoplasmic Shuttling of Protons in *Anabaena* Sensory Rhodopsin: Implications for Signaling Mechanism. *J. Mol. Biol.* **2006**, *358*, 686−700.

(10) Wand, A.; Rozin, R.; Eliash, T.; Jung, K. H.; Sheves, M.; Ruhman, S. Asymmetric Toggling of a Natural Photoswitch: Ultrafast Spectroscopy of *Anabaena* Sensory Rhodopsin. *J. Am. Chem. Soc.* **2011**, *133*, 20922−20932.

(11) Kalisky, O.; Goldschmidt, C. R.; Ottolenghi, M. On the Photocycle and Light Adaptation of Dark-adapted Bacteriorhodopsin. *Biophys. J.* **1977**, *19*, 185−189.

(12) Furutani, Y.; Kawanabe, A.; Jung, K. H.; Kandori, H. FTIR Spectroscopy of the All-trans Form of *Anabaena* Sensory Rhodopsin at 77K: Hydrogen Bond of a Water between the Schiff Base and Asp75. *Biochemistry* **2005**, *44*, 12287−12296.

(13) Kawanabe, A.; Furutani, Y.; Jung, K. H.; Kandori, H. FTIR Study of the Photoisomerization Processes in the 13-*cis* and All-*trans* Forms of *Anabaena* Sensory Rhodopsin at 77 K. *Biochemistry* **2005**, *45*, 4362−4370.

(14) Sineshchekov, O. A.; Spudich, J. L. Light-induced Intramolecular Charge Movements in Microbial Rhodopsin in Intact *E. coli* Cells. *Photochem. Photobiol. Sci.* **2004**, *3*, 548−554.

(15) Sineshchekov, O. A.; Spudich, E. N.; Trivedi, V. D.; Spudich, J. L. Role of the Cytoplasmic Domain in *Anabaena* Sensory Rhodopsin Photocycling: Vectoriality of Schiff Base Deprotonation. *Biophys. J.* **2006**, *91*, 4519−4527.

(16) Bergo, V. B.; Ntefidou, M.; Trivedi, V. D.; Amsden, J. J.; Kralj, J. M.; Rothschild, K. J.; Spudich, J. L. Conformational Changes in the Photocycle of *Anabaena* Sensory Rhodopsin Absence of the Schiff Base Counterion Protonation Signal. *J. Biol. Chem.* **2006**, *281*, 15208−15214.
(17) Kawanabe, A.; Furutani, Y.; Yoon, S. R.; Jung, K. H.; Kandori, H. FTIR Study of the L Intermediate of *Anabaena* Sensory Rhodopsin: Structural Changes in the Cytoplasmic Region. *Biochemistry* **2008**, *47*, 10033−10040.
(18) Kondoh, M.; Inoue, K.; Sasaki, J.; Spudich, J. L.; Terazima, M. Transient Dissociation of the Transducer Protein from *Anabaena* Sensory Rhodopsin Concomitant with Formation of the M State Produced upon Photoactivation. *J. Am. Chem. Soc.* **2011**, *133*, 13406−13412.
(19) Wada, Y.; Kawanabe, A.; Furutani, Y.; Kandori, H.; Ohtani, H. Quantum Yields for the Light Adaptations in *Anabaena* Sensory Rhodopsin and Bacteriorhodopsin. *Chem. Phys. Lett.* **2008**, *453*, 105−108.
(20) Kawanabe, A.; Furutani, Y.; Jung, K. H.; Kandori, H. Photochromism of *Anabaena* Sensory Rhodopsin. *J. Am. Chem. Soc.* **2007**, *129*, 8644−8649.
(21) Strambi, A.; Durbeej, B.; Ferre, N.; Olivucci, M. *Anabaena* Sensory Rhodopsin is a Light-Driven Unidirectional Rotor. *Proc. Natl. Acad. Sci. U.S.A.* **2010**, *107*, 21322−21326.
(22) Honig, B.; Greenberg, A. D.; Dinur, U.; Ebrey, T. G. Visual-pigment Spectra: Implications of the Protonation of the Retinal Schiff Base. *Biochemistry* **1976**, *15*, 4593−4599.
(23) Honig, B.; Dinur, U.; Nakanishi, K.; Balogh-Nair, V.; Gawinowicz, M. A.; Arnaboldi, M.; Motto, M. G. An External Point-charge Model for Wavelength Regulation in Visual Pigments. *J. Am. Chem. Soc.* **1979**, *101*, 7084−7086.
(24) Nakanishi, K.; Balogh-Nair, V.; Arnaboldi, M.; Tsujimoto, K.; Honig, B. An External Point-charge Model for Bacteriorhodopsin to Account for its Purple Color. *J. Am. Chem. Soc.* **1980**, *102*, 7945−7947.
(25) Houjou, H.; Inoue, Y.; Sakurai, M. Study of the Opsin Shift of Bacteriorhodopsin: Insight from QM/MM Calculations with Electronic Polarization Effects of the Protein Environment. *J. Phys. Chem.* **2001**, *105*, 867−879.
(26) Melaccio, F.; Ferre, N.; Olivucci, M. Quantum Chemical Modeling of Rhodopsin Mutants Displaying Switchable Colors. *Phys. Chem. Chem. Phys.* **2011**, *14*, 12485−12495.
(27) Oesterhelt, D.; Stoeckenius, W. Rhodopsin-like Protein from the Purple Membrane of *Halobacterium halobium*. *Nat. New Biol.* **1971**, *233*, 149−152.
(28) Kobayashi, T.; Ohtani, H.; Iwai, J.; Ikegami, A.; Uchiki, H. Effect of pH on the Photoreaction Cycles of Bacteriorhodopsin. *FEBS Lett.* **1983**, *162*, 197−200.
(29) Ohtani, H.; Kobayashi, T.; Iwai, J. Picosecond and Nanosecond Spectroscopies of the Photochemical Cycles of Acidified Bacteriorhodopsin. *Biochemistry* **1986**, *25*, 3356−3363.